Research Center for Molecular Materials

VIII-C Development of Novel Heterocyclic Compounds and Their Molecular Assemblies for Advanced Materials

Heterocycles containing sulfur and/or nitrogen atoms are useful as components of functional materials since heteroatoms in their rings are helpful to stabilize ions or ion-radical species, and extended π-conjugation decreases Coulombic repulsion. In addition intermolecular interactions caused by heteroatom contacts can be expected to form novel molecular assemblies. In this project new electron acceptors, donors, and donor-acceptor compounds based on heterocycles such as 1,2,5-thiadiazole and 1,3-dithiole were synthesized and their properties including those of the charge-transfer complexes or ion-radical salts were investigated. Unique crystal structures were constructed by using weak intermolecular interactions such as hydrogen bonding or heteroatom contacts. Heterocyclic oligomers with rigid structures were also synthesized for molecular wires.

VIII-C-1 Preparation of New TTF Vinylogues Containing Substituents at the Vinyl Positions

YAMASHITA, Yoshiro; TOMURA, Masaaki

TTF vinylogues **1** have a stronger electron-donating ability and reduced on-site Coulomb repulsion owing to the extended π-delocalized system. The physical properties and structures can be tuned by the substituents at the vinyl positions. For example the ortho-substituted phenyl groups can keep the TTF vinylogue skeleton plane by taking twisting conformations, leading to the stable cation radical states.[1)] We have now prepared the new derivatives **1** and **2**, and investigated their properties. New compounds **1a–d** possess cyano or bromo substituents which can induce intermolecular interactions. The synthesis is based on oxidative coupling reaction of the corresponding 1,4-dithiafulvenes. **1e** with 2-pyridyl substituents and **1f** with phenylethynyl groups were also synthesized. **1f** has no steric hindrance caused by substituents. Furthermore, we have obtained cyclophane-type molecules **2** which have a bridge between the phenyl substituents. The following oxidation potentials of new molecules were observed. **1a**; 0.61, 0.84, **1b**; 0.64 (2e), **1c**; 0.51, 0.75, **1d**; 0.68 (2e), **1e**; 0.91 (irrev.), **1f**; 0.57, 0.76, **2a**; 0.48, 0.64, **2b**; 0.52, 0.65; **2c**; 0.40, 0.63V *vs.* SCE.

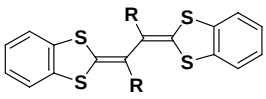

1a; R = *o*-CNC_6H_4
1b; R = *p*-CNC_6H_4
1c; R = *o*-BrC_6H_4
1d; R = *p*-BrC_6H_4
1e; R = 2-Pyridyl
1f; R = PhC C-

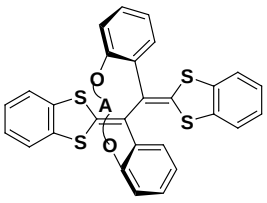

2a; A = CH_2CH_2
2b; A = CH_2SCH_2
2c; A = $(CH_2)_4$

Reference

1) Y. Yamashita, M. Tomura, M. B. Zaman and K. Imaeda, *Chem. Commun.* 1657 (1998).

VIII-C-2 Preparation, Structure, and Properties of 1,3-Bis(1,4-dithiafulven-6-yl)azulenes

OHTA, Akira[1]; YAMAGUCHI, Kyoko[1]; FUJISAWA, Naoki[1]; YAMASHITA, Yoshiro; FUJIMORI, Kunihide[1]

([1]Shinshu Univ.)

Novel bis(1,3-dithiole) electron donors **1** containing an azulene spacer unit were prepared from 1,3-diformylazulene using a Wittig-Horner reaction in 20-85% yields. The first oxidation potentials of **1** are lower than that of TTF, indicating that they are stronger donors than TTF as predicted by the PM3 calculations. In addition to the oxidation waves, they show an irreversible reduction peak at *ca.* –1.4 V. This amphoteric nature is consistent with the absorption data where the longest absorption maxima are observed at 733–762 nm in dichloromethane. The structure features of a benzo-fused derivative were investigated by X-ray analysis. One of the 1,4-dithiafulvenyl groups and the azulene moiety are in almost coplanar, while the other one twists with a torsion angle of 20.8°. The spectroelectrochemical studies on the methylthio derivative reveals that the cation radical and dication state have the longest absorption maxima at 612 and 721 nm, respectively.

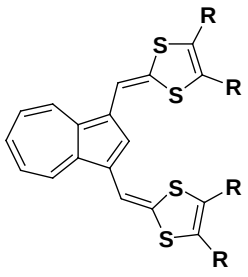

R = H, SMe, SCH_2CH_2S, $(CH=CH)_2$

1

VIII-C-3 Synthesis and Characterization of Novel Strong Electron Acceptors: Bithiazole Analogues of Tetracyanodiphenoquinodimethane (TCNDQ)

SUZUKI, Kazuharu; TOMURA, Masaaki; TANAKA, Shoji; YAMASHITA, Yoshiro

Pyridine analogues of TCNQ are unstable due to the much stronger electron accepting ability. On the other hand, thiophene-TCNQs are generally weak electron acceptors due to the electron donating effect of the thiophene ring. Therefore, we have designed a new

electron acceptor **1**, a TCNDQ analogue containing Nitrogen and Sulfur atoms in the skeleton. **1** was prepared by using Pd-catalyzed coupling reaction of dicyanomethanide to a dibromo precursor **4**. The new acceptor shows a strong electron accepting ability and small on-site Coulomb repulsion. The methoxy derivatives **2** and **3** were also obtained by substitution reaction of **1** with methanol. The reduction potentials of **2** and **3** are lower than that of **1** due to the electron donating methoxy substituents. The X-ray analysis of **1** and **2** has revealed the planar structures containing a double bond with *E*-configuration. The acceptors **1**–**3** have characteristic strong absorptions around 550 nm. **1** afforded several charge transfer complexes with electron donors such as TTF.

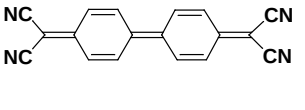

TCNDQ

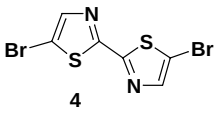

4

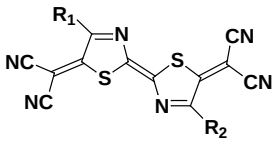

1; $R_1 = R_2$ =H
2; R_1 = H, R_2 = OMe
3; $R_1 = R_2$ = OMe

VIII-C-4 Heterocyclic TCNQ Analogues Containing Thiophene and Benzothiadiazole Units

SUZUKI, Kazuharu; TOMURA, Masaaki; YAMASHITA, Yoshiro

Sulfur containing TCNQ analogues are highly polarized and are expected to have strong intermolecular interactions by heteroatom contacts. We have recently prepared a TCNDQ derivative **1** containing fused thiadiazole rings. As an extension of this work, we have now prepared new π-extended electron acceptors **2** and **3** composed of benzothiadiazole and thiophene units. They were synthesized using the Pd catalyzed reaction of the corresponding dibromides **4** and **5** with malononitrile anion. The absorption maxima of **2** and **3** were observed at 524 and 635 nm in dichloromethane, respectively. **2** shows stepwise one-electron reduction waves at +0.07 and –0.17 V *vs.* SCE, while **3** shows a one-step two-electron reduction wave at +0.08 V *vs.* SCE. The values of the first reduction potentials are lower than that of TCNQ, indicating that they are not so strong acceptors. However, they are still stronger acceptors than the corresponding thiophene-TCNQ analogues. The X-ray analysis revealed that **2** has a planar geometry and the central double bond takes a Z-configuration. **2** gave various charge transfer complexes and anion radical salts. The Me_4P^+ salt exhibits a high conductivity of 8.4 Scm^{-1}.

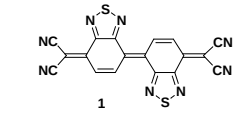

1

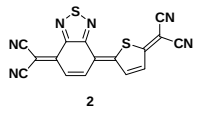

2

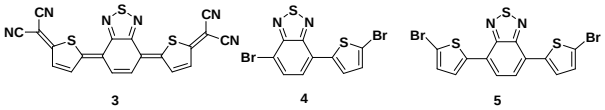

3 **4** **5**

VIII-C-5 Crystal Engineering in π-Overlapping Stacks: Unusual One- and/or Two-Dimensional Stacking of π-System in the Crystal Structure of the Cation Radical Salts of Tetrathiafulvalene Vinylogues

TOMURA, Masaaki; YAMASHITA, Yoshiro

[*CrystEngComm* 14 (2000)]

One- and/or two-dimensional π-overlapping stacks have been found in the crystals of the cation radical salts of the tetrathiafulvalene vinylogues **1** and **2** having *o*-substituted phenyl groups at the vinyl positions. The packing mode in the two-dimensional π-stacks could be modified depending on the counter anions. We have observed the pseudo two-dimensional stacking and the zigzag two-dimensional stacking with an angle of nearly 90° in the crystal structure of **1**–$FeCl_4$ and **1**–ReO_4 salts, respectively. In the case of **2**–PF_6–$(H_2O)_8$ salt, we have observed not the two-dimensional π–π overlapping stack found in the cation radical salts of **1**, but the one-dimensional stacking of π-system. The one-dimensional overlapping mode of **2** has brought a square grid-like structure (Figure 1) with a void in which eight water molecules are occupied. The 1,3-dithiole rings in **2** are unfavorable for π-π intermolecular interactions due to the less π-delocalization and steric interactions of the ethylenedithio parts compared to those in **1**. This seems to lead to the novel one-dimensional structure, not the two-dimensional one.

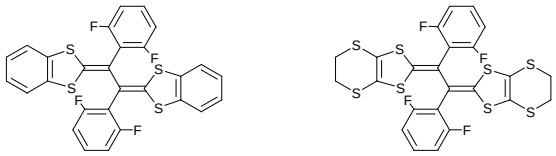

1 **2**

Figure 1. Crystal structure of **2**–PF_6–$(H_2O)_8$ salt viewed along the *c* axis. The water molecules are omitted for clarity.

VIII-C-6 One-Dimensional Supramolecular Tapes in the Co-Crystals of 2,5-Dibromo-3,6-dihydroxy-1,4-benzoquinone (Bromanilic Acid) with Heterocyclic Compounds Containing a Pyrazine Ring Unit

TOMURA, Masaaki; YAMASHITA, Yoshiro

[*CrystEngComm* 16 (2000)]

The design of new molecular architectures for crystal engineering has generated great interest in recent years. We have carried out co-crystallization of 2,5-dibromo-3,6-dihydroxy-1,4-benzoquinone (bromanilic acid) with heterocyclic aromatic compounds, phenazine, quinoxaline and pyrazine. The X-ray crystallographic analyses of the co-crystals suggest the supramolecular synthon formed with bromanilic acid and the heterocyclic compounds can yield the robust one-dimensional supramolecular tapes (Figure 1) and realize preserved interesting crystal structures.

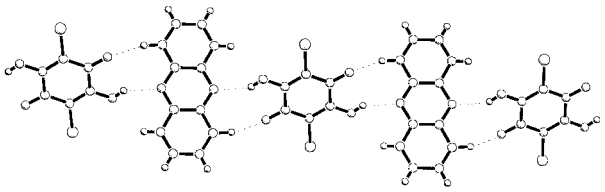

Figure 1. One-dimensional tape in the co-crystal of bromanilic acid with phenazine.

VIII-C-7 A Decamethylferrocene [$Fe(C_5Me_5)_2$] and Chloranilic Acid (CA) Complex with Hydrogen Bonded Supramolecular Structure between CA and H_2O

ZAMAN, Md. Badruz; TOMURA, Masaaki; YAMASHITA, Yoshiro; SAYADUZZAMAN, Md.[1]; CHOWDHURY, A. M. Sarwaruddin[1]
([1]Dhaka Univ.)

[*CrystEngComm* 9 (1999)]

The chloranilic acid as acceptor (A) has been used to prepare crystalline materials with organometallic decamethylferrocene as donor (D). The structure was obtained by single crystal X-ray analysis and the stoichiometric ratio [D:A:H_2O = 1:1:1] was confirmed by elemental analysis. These analyses reveal the molecular complex as $[Fe(C_5Me_5)_2]^+[CA]^-[H_2O]$. The water molecules in this crystal act as cohesive elements by connecting the anions through O–H··O hydrogen bonds to form an infinite one-dimensional supramolecular structure along the b axis (Figure 1). This solid-state structural aspects of DA solids has interesting, highly charged ground states, which are not commonly observed in $Fe(C_5Me_5)_2$ complexes due to the paucity of stability and highly charged species.

Figure 1. View of the hydrogen bonded network with CA and H_2O molecule.

VIII-C-8 New Hydrogen Bond Donor-Acceptor Pairs between Dipyridylacetylenes and 2,5-Dichloro-3,6-dihydroxy-1,4-benzoquinone

ZAMAN, Md. Badruz; TOMURA, Masaaki; YAMASHITA, Yoshiro

[*Org. Lett.* **2**, 273 (2000)]

The crystalline donor-acceptor hydrogen bonding complexes between 2,5-chloro-3,6-dihydroxy-1,4-benzoquinone (chloranilic acid, H_2CA) and dipyridyl-acetylenes (DPA) [2,2'-DPA, 3,3'-DPA and 4,4'-DPA] were prepared and crystal structures were revealed by X-ray analysis. The structures of the complexes are formed by intermolecular hydrogen bonding interactions and demonstrate three beautiful supramolecular architectures based on a new common supramolecular synthon (Figure 1), which allows controlling the crystal structures, ionicity and stacking arrangements.

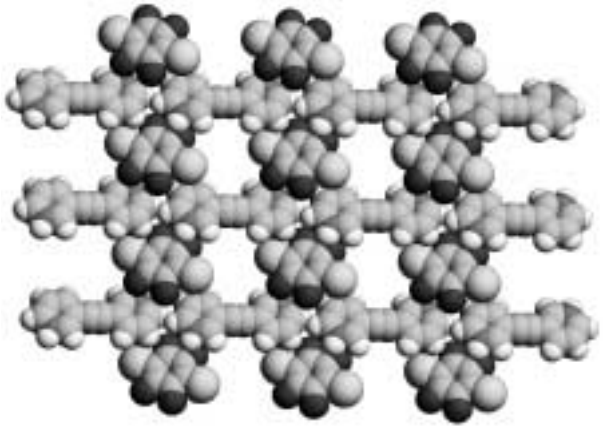

Figure 1. Square grids structure of $[CA]^{2-}[3,3'\text{-}H_2DPA]^{2+}\text{-}(H_2O)_{3.3}$ complex. The water molecules are omitted for clarity.

VIII-C-9 Novel Synthetic Approach to 5–10 nm Long Functionalized Oligothiophenes

TANAKA, Shoji ; YAMASHITA, Yoshiro

The development of precisely-defined oligomers with extended π-conjugation length comparable to the inter-electrode gap currently made by nano-patterning techniques (5~10 nm gap) has generated a great deal of interest. The reason for this is that highly oligomers of this class will become an important tool for providing specific information on the parameters controlling the long-distance electron-tunneling through a single molecular wire. Here we will report a new synthetic approach to a series of precisely defined 5–10 nm long oligothiophenes, using N-silyl-protected 3,4-

diaminothiophene as a key building unit. Scheme 1 shows the synthetic pathways for α-14T (**3**: l ~ 5 nm) and α-28T (**5**: l ~ 10 nm) derivatives. Purification of all oligomers (**1**–**5**) was achieved by preparative gel permeation chromatography, and the purity was clearly revealed by MALDI-TOF mass spectrometry in the positive ion and linear detection mode using dithranol as matrix. The desilylation and further chemical modifications of the N-silyl-protected 3,4-diaminothiophene moieties of the obtained oligomers will afford various types of 5–10 nm long functionalized oligomers.

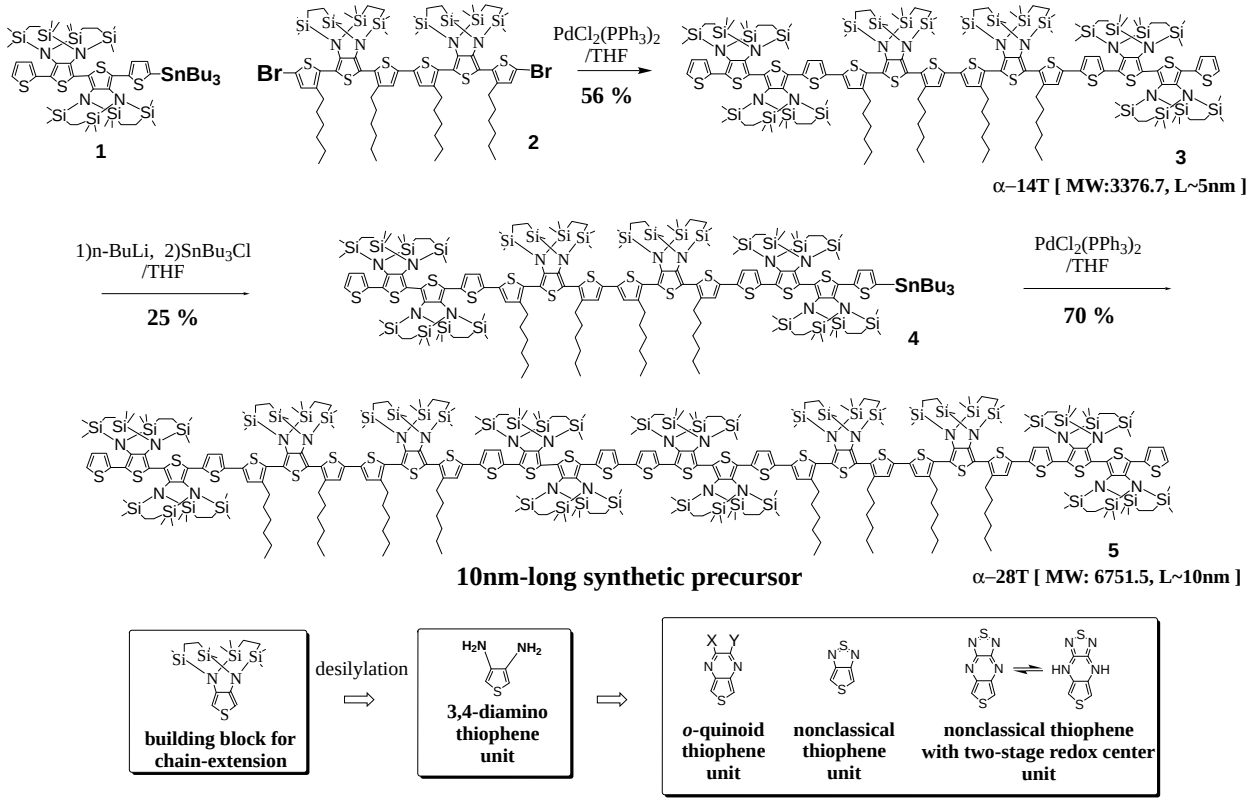

Scheme 1.

VIII-D Elecrtonic Structures and Rectivities of Active Sites of Metalloproteins

Metalloproteins are a class of biologically important macromolecules which have various functions such as oxygen transport, electron transfer, oxidation, and oxygenation. These diverse functions of metalloproteins have been thought to depend on the ligands from amino acid, coordination structures, and protein structures in immediate vicinity of metal ions. In this project, we are studying the relationship between the structures of the metal active sites and functions of metalloproteins.

VIII-D-1 Resonance Raman Spectra of Legitimate Models for the Ubiquitous Compound I Intermediates of Oxidative heme Enzymes

CZARNECKI, Kazimierz[1]; KINCAID, James R.[1]; FUJII, Hiroshi
([1]Marquette Univ.)

[*J. Am. Chem. Soc.* **121**, 7953 (1999)]

Resonance Raman (RR) spectra are reported for two models of the compound I intermediates of oxidative heme proteins; namely, the imidazole (Im) and 2-methyl-imidazole (2-MeIm) complexes of the ferryl π-cation radical derivative of iron-(5,10,15,20-tetra-mesitylporphyrin), $[O=Fe(TMP^{+\bullet})(Im)]^+$ and $[O=Fe(TMP^{+\bullet})]^+$, which are stablized in dichloromethane solution at –80 °C. The present study yields high quality RR spectra of these complexes and provides the forst opportunity to compare the ν(Fe=O) stretching modes and the structure-sensitive core maker modes for a ferrylporphyrin π-cation radical with the corresponding modes of the neutral parent bearing the same trans-axial ligand. While the observed shifts in the frequencies of the core modes are in agreement with those expected upon formation of the π-cation radical, the results suggest that the isolated effect of macrocycle oxidation on the Fe=O stretching frequency is rather small; the observed shift being only about 4 cm^{-1} to lower frequency.

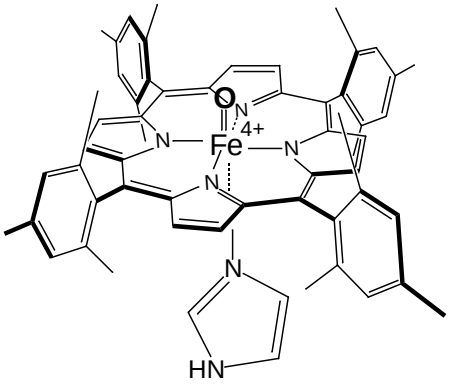

Figure 1. Structure of model complexes of the compounds I of oxidative heme proteins.

VIII-D-2 Spin Distribution in Low-Spin (meso-Tetraalkylporphyrinato)iron(III) Complexes with $(dxz,dyz)^4$ $(dxy)^1$ Configuration. Studies by ^{1}H-NMR, ^{13}C-NMR, and EPR Spectroscopies

IKEUE, Takahisa[1]; OHGO, Yoshiki[1]; SAITOH, Takashi[1]; NAKAMURA, Mikio[1]; FUJII, Hiroshi; YOKOYAMA, Masataka[2]
([1]Toho Univ. Sch. Med.; [2]Chiba Univ.)

[*J. Am. Chem. Soc.* **122**, 4068 (2000)]

^{1}H-NMR, ^{13}C-NMR, and EPR studies of a series of low-spin (meso-tetraalkylporphyrinato)iron(III) complexes, $[Fe(TRP)(L)_2]X$ where R = n-Pr, c-Pr, and i-Pr and L represents axial ligands such as imidazoles, pyridines, and cyanide, have revealed that the ground-state electron configuration of $[Fe(TnPrP)(L)_2]X$ and $[Fe(TcPrP)(L)_2]X$ is presented either as the common $(dxy)^2$ $(dxz,dyz)^3$ or as the less common $(dxz,dyz)^4$ $(dxy)^1$ depending on the axial ligands. The ground-state electron configuration of the isopropyl complexes $[Fe(Ti\text{-}PrP)(L)_2]X$ is, however, presented as $(dxz,dyz)^4$ $(dxy)^1$ regardless of the kind of axial ligands. In every case, the contribution of the $(dxz,dyz)^4$ $(dxy)^1$ state to the electronic ground state increases in the following order: HIm < 4-Me_2NPy < 2-MeIm < CN^- < 3-MePy < Py < 4-CNPy. Combined analysis of the ^{13}C and ^{1}H NMR isotropic shifts together with the EPR *g* values have yielded the spin densities at the porphyrin carbon and nitrogen atoms. Estimated spin densities in $[Fe(TiPrP)(4\text{-}CNPy)_2]^+$, which has the purest $(dxz,dyz)^4$ $(dxy)^1$ ground state among the complexes examined in this study, are as follows: meso-carbon, +0.045; β-pyrrole carbon, +0.0088; α-pyrrole carbon, –0.00026; and pyrrole nitrogen, +0.057. Thus, the relatively large spin densities are on the pyrrole nitrogen and meso-carbon atoms. The result is in sharp contrast to the spin distribution in the $(dxy)^2$ $(dxz,dyz)^3$ type complexes; the largest spin density is at the α-pyrrole carbon atoms in bis(1-methylimidazole)(meso-tetraphenylporphyrinato)-iron(III), $[Fe(TPP)(1\text{-}MeIm)_2]^+$, as determined by Goff. The large downfield shift of the meso-carbon signal, ä +917.5 ppm at –50 °C in $[Fe(TiPrP)(4\text{-}CNPy)_2]^+$, is ascribed to the large spin densities at these carbon atoms. In contrast, the large upfield shift of the β-pyrrole carbon signal, –293.5 ppm at the same temperature, is caused by the spin polarization from the adjacent meso-carbon and pyrrole nitrogen atoms.

VIII-D-3 Post-Assembly Insertion of Metal Ions into Thiol-Derivatized Porphyrin Monolayers on gold

NISHIMURA, Noboru[1]; OOI, Masanori[1]; SHIMATZU, Katsuaki[1]; FUJII, Hiroshi; UOSAKI, Kohei[1]
([1]Hokkaido Univ.)

[*J. Electro. Chem.* **473**, 75 (1999)]

The insertion of metal ions into thiol-derivatized free base porphyrin monolayers pre-assembled on gold has been conducted by refluxing the metal ion solution in which the monolayer-coated gold electrode was immersed. The extend of the metal insertion was estimated from the decrease in the N1s peaks in X-ray photoelectron spectra (XP spectra) assigned to the pyrrole nitrogen which binds a hydrogen atoms. The insertion of Co(II) was completed by refluxing for 3 hr. Although the extent of the metal insertion for the same reflux time depends on the metal ion used, the insertion of several ions including Mn(II), Fe(II), Ni(II), Cu(II) and Zn(II) was possible. Besides XP spectra, the metal insertion was confirmed by the electrocatalytic activity of the monolayers for the reduction of molecular oxygen. The structural characterization has proved that the monolayer is stable during the reflux: neither desorption nor change in the orientation of the porphyrin molecules took place. Compared to the commonly used self-assembly of the pre-metalated porphyrin, this post-assembly metal insertion method has an advantage because neither intra nor intermolecular coordinations of the thiol functionality to the central metal ion take place, thus avoiding the unexpected disorder in the monolayer such as the formation of a multilayer, the blocking of the electrocatalytically active metal ion and loss of the anchoring functionality or thiol.

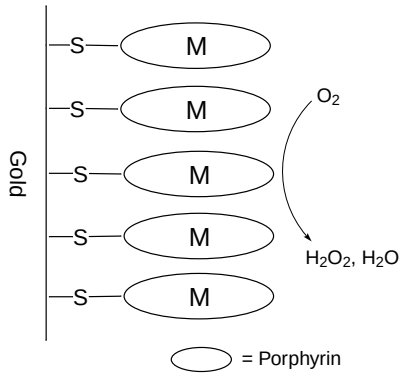

Figure 1. Porphyrin monolayer formed by the self-assemble on gold surface.

VIII-D-4 Electron Spin-Echo Envelope Modulation Spectral properties of Amidate Nitrogen Coordinated to Oxovanadium(IV) Ion

FUKUI, Koichi[1]; FUJII, Hiroshi; OHYA-NISHIGUCHI, Hiroaki[1]; KAMADA, Hitoshi[1]
([1]Inst. Life. Supp. Tech.)

[*Chem. Lett.* 198 (2000)]

Increse evidence shows that vanadium palys a variety of roles in biological systems. For instance, a class of haloperoxidase requires vanadium for their enzymatic activities. Vanadium is also know to have beneficial insulin-mimetic activities, and some vanadium complexes are studied as a candidate for an orally-active anti-diabetic agent. These findings have stimulated interests in the interactions of vanadium with biological substances such as an amnio acids, peptides, and proteins. In the stduies on this subject, interests are often focused on carboxylate, imidazole and amino groups for vanadium-coordinating groups. However, recent studies have shown that amido group can undergo reprotonation/coordination reaction even at physiological conditions when an anchoring group is present. Therefore, it is possible that vanadium-amidate bonding actually ocuurs and plays some roles in biological systems. For characterization of vanadium(IV) cooridnation environments, electron spin-echo envelope modulation (ESEEM) spectroscopy is suited. It has been demonstrated that ESEEM results not only reveal the presence or absence of nitrogen nuclei coordinated to VO^{2+} ion (and possibly the number of the coordinating nitrogen atoms), but allow identification of equatorial nitrogens based on the emprirical correlation between the type of the nitrogen and the ^{14}N hyperfine coupling (HFC) parameter. However, neither the HFC parameters nor the nuclear quadropole coupling (NQC) pararmeters are known for vanadium-coordinated amidataed nitrogens. Here we report the first ESEEM results for a structurally-characterized VO^{2+}-amidate complex.

VIII-D-5 Newly Designed Iron-Schiff Base Complexes as Models of Mononuclear Non-Heme Iron Active Sites

FUNAHASHI, Yasuhiro; FUJII, Hiroshi

High valent iron-oxo species have been suggested as the active intermediates for catalytic oxygenation reactions by iron-containing oxygenases. In the reaction mechanisms of heme and binuclear non-heme iron enzymes, an Fe^{IV}=O porphyrin radical species (Compound I) and a $Fe^{IV}_2(m\text{-}O)_2$ species (Intermediate Q) have been found to be responsible oxidant for alkane hydroxylation and alkene epoxidation. Such the high valent iron-oxo species are inferred to involve in hydroxylation of aromatic compounds by mononuclear non-heme iron oxygenases, the reaction processes of which, however, still remains to be established. In order to gain insight into the active intermediates, we try to synthesize iron complexes with bulky schiff-base ligands as biomimetic models of mononuclear non-heme iron active sites. The active oxygen adduct of these complexes, which would be kinetically stabilized by their steric hindrance, might provide a basis for understanding the oxygenation by mononuclear iron sites.

VIII-D-6 Synthesis and Characterization of High Valent Iron Porphyrin Complexes as Models for Reaction Intermediates of Cytochrome *c* Oxidase

IKEUE, Takahisa; FUMOTO, Yumiko[1]; ONO, Noboru[1]; FUJII, Hiroshi
([1]Ehime Univ.)

Cytochrome c oxidase is the terminal oxidase which reduces molecular oxygen (O_2) to water (H_2O), coupling with proton pumping across the mitochondrial inner membrane. Since discovery of this enzyme, many

structural and functional studies have been done to understand its reaction mechanism. Recent X-ray analyses reveal that this enzyme contains a binuclear center, heme-a_3-Cu_B site, as a reaction site in the catalytic core, and Cu_A and Heme-a as electron transfer sites in the backbone structure, respectively. The binuclear center of the resting enzyme is ferric/cupric form. The binuclear active site is reduced to a ferrous/cuprous form by two electrons from cytochrome c through the Cu_A and heme a site. The ferrous/cuprous form of active site reacts with O_2 to yield an internal dioxygen adduct, intermediate A state, which is further converted to intermediate P and F by the aid of the electrons and protons. Although the intermediates P and F have been studied by resonance Raman and flash-flow absorption spectroscopies, the electronic states of these intermediates are not still clear. To reveal the electronic states of these intermediates and to understand the reaction mechanism of cytochrome c oxidase, we have synthesized model complexes of the heme-a_3 site of cytochrome *c* oxidase. The model complex contains a formyl group at pyrrole-β position to mimic the heme a_3 and mesityl groups to stabilize high valent oxo iron species. We have succeeded in the preparation of a high valent oxo iron porphyrin complex as a model for the intermediate P by the oxidation of the ferric model complex with mCPBA or ozone.

VIII-E Molecular Mechanism of Heme Degradation and Oxygen Activation by Heme Oxygenase

Heme oxygenase (HO), an amphipathic microsomal proteins, catalyzes the regiospecific oxidative degradation of iron protoporphyrin IX (heme) to biliverdinIXα, carbon monoxide, and iron in the presence of NADPH-cytochrome P-450 reductase, which functions as an electron donor. Heme oxygenase reaction is the biosynthesis processes of bile pigments and CO which is a possible physiological messenger. Recent development in the bacterial expression of a soluble form of heme oxygenase has made it possible to prepare in the large quantities for structural studies. In this project, we are studying the molecular mechanism of heme degradation and the oxygen activation by heme oxygenase using various spectroscopic methods.

VIII-E-1 Participation of Carboxylate Amino Acid Side Chain in Regiospecific Oxidation of Heme by Heme Oxygenase

ZHOU, Hong[1]; MIGITA, Taiko Catharine[2]; SATO, Michihiko[1]; SUN, Donghu[1]; ZHANG, Xuhong[1]; IKEDA-SAITO, Masao[2]; FUJII, Hiroshi; YOSHIDA, Tadashi[1]

([1]Yamagata Univ. Sch. Med.; [2]Yamaguchi Univ.; [3]Case West. Res. Univ. Sch. Med.)

[*J. Am. Chem. Soc.* **122**, 8311 (2000)]

The regioselective oxidation of the α-meso position by HO is quite unique, in contrast to the non-enzymatic heme degradation that forms a mixture of four possible α, β, γ, δ-biliverdin isomers. The present study shows the first evidence of the formation of biliverdin isomers other than biliverdinIXα by HO mutants. The replacement of the highly conserved arginine 183(R183) of HO-1 with glutamic acid (E) or aspartic acid (D) forms biliverdinIXδ isomer along with normal biliverdinIXα. The absorption and EPR spectra and HO catalytic activity of R183E mutant are similar to those of the wild type heme-HO complex, indicating no significant change in the active site structure with mutation. To investigate the effects of the carboxylate functionalities introduced at the position 183, we prepared R183Q, R183N, R183A, R183T, and R183Y. The HO reactions of these mutants do not produce biliverdin isomers other than the normal biliverdinIXα. These results indicate that the carboxylate group introduced at position 183 is involved in the formation of δ-biliverdin isomer. The formation of δ-biliverdin isomer is expected to result in heme rotation through electronic repulsion between the carboxylate of E183 and heme propionate and/or change in distal side protein structure through a formation of new long-range hydrogen bond interaction network. All of the present results show the importance of the hydrogen bonding interaction between the arginine at position 183 and the carboxylates of the heme propionate group, as well as steric effect of the distal helix, for the α-regioselectivity.

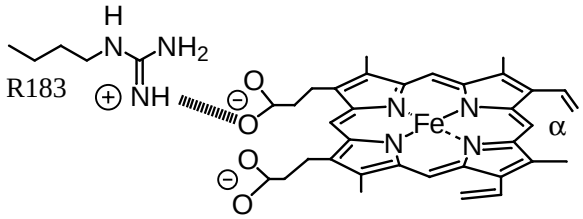

Figure 1. The hydrogen bonding interaction between R183 residue and the carboxylate of heme orients the heme to oxidize the α-meso position.

VIII-F Designing Artificial Photosynthesis at Molecular Dimensions

Photosynthesis is one of the finest piece of molecular machinery that Nature has ever created. Its ultrafast electron transfer and following well-organized sequence of chemical transformation have been, and will continue to be, challenging goals for molecular scientists. We are trying to mimic the function of photosynthesis by assembling molecular units that perform individual physical/chemical action. The molecular units include porphyrins, redox active organic molecules, and transition metal complexes.

Last year we focused our attention on developing organic reactions that utilize photoinduced electron transfer processes and are useful for synthetic organic chemistry. This is an important step toward our ultimate goal, which is to design artificial molecular systems that effect multiple chemical reactions triggered by light on the basis of molecular rationale.

VIII-F-1 Porphyrin Catalyzed Reductive Silylation and Acylation of Quinones under Irradiation of Visible Light

ITO, Hajime; NAGATA, Toshi

Considerable studies were reported for inter- or intramolecular photoinduced electron transfer from porphyrins to quinones, however, the synthetic application of a porphyrin as a photocatalyst for the reduction of quinones is thought to be still difficult. For example, when attempts to obtain the reduced products of a quinone was carried out using a porphyrin catalyst under irradiation of visible light in the presence of a proton source, no reduced products were detected. The reason for this unsuccessful result would be mainly attributed to the reverse electron transfer from a semiquinone anion radical to the porphyrin cation radical generated by the photoinduced electron transfer. If the semiquinone anion radical is chemically trapped by a silyl reagent and the successive silylation occurs, the reductive silylation product of the quinone is obtained. On the basis of this idea, we found both phenylthiotrimethylsilane (PhSTMS) and chlorotrimethylsilane (TMSCl) are a good trapping reagent for the reduced intermediate formed by photoinduced electron transfer from photo-excited porphyrins. In addition, the electrophilic substitution of a silyl sulfide with a phenoxy group releases a thiolate anion which would act as an electron donor. In the presence of a catalytic amount of porphyrin **1** (0.5 mol %), the reductive silylation of duroquinone was proceded under the irradiation of yellow light ($\lambda > 500$ nm) using PhSTMS to give 1,4-bis(trimethylsiloxy)-2,3,5,6-tetramethylbenzene (99%) and diphenyl disulfide (97%) in good yields. We also found that chlorotrimethylsilane (TMSCl), a more easily available silyl reagent, was also useful for the porphyrin-catalyzed reductive silylation.

Despite the reductive silylation and acylation of quinones with chlorotrimethylsilane and metal (K, Mg, Zn) were well known procedure, these methods require a stoichiometric amount of metals as a reductant and generate waste metal salt. Our method exhibit the practical advantage in view of this points. Further work on the precise mechanism for these reactions is underway.

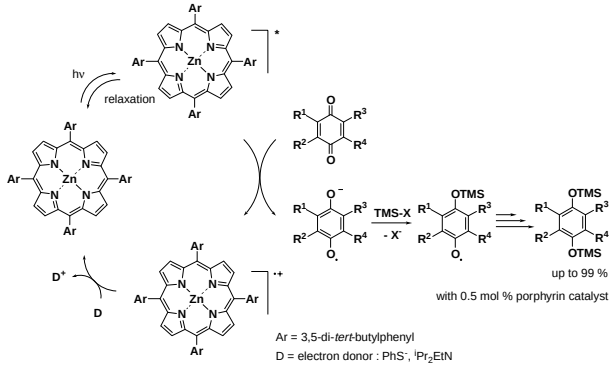

Figure 1. Porphyrin-catalyzed silylation of quinones under visible light.

VIII-G Development of New Metal Complexes as Redox Catalysts

Redox catalysis is an important field of chemistry which translates a flow of electron into chemical transformation. It is also one of the requisites for artificial photosynthesis. This project of ours aims at developing new metal complexes that perform redox catalysis at low overpotential. Our approach is to develop a series of "binary" ligands, which consist of two different types of ligands that are linked together to form metal chelates. Such ligands are particularly useful for utilizing first-row transition metal elements, because fast ligand exchange (which is often a major obstacle in studying first-row transition metal complexes in solution) is suppressed by chelate effects.

VIII-G-1 Synthesis of Terpyridine-Based Binary Ligands and Their Metal Complexes

[*Inorg. Chem.* **39**, 3515 (2000)]

NAGATA, Toshi; TANAKA, Koji

2,2':6',2"-Terpyridine is a promising ligand for application in redox catalysis, thanks to its structural

rigidity and chemical stability. Unfortunately, with first-row transition metals it easily forms homoleptic bis(terpyridine) complexes that are too stable to serve as redox catalysts. Such difficulty can be overcome by connecting a bidentate ligand to a terpyridine molecule. The "binary" ligand thus formed is potentially pentadentate and binds an octahedral metal ion leaving one vacant site for catalytic reactions. We already reported synthesis of terpyridine-catechol linked ligands and their cobalt(III) complexes (Figure 1a). Here we report synthesis of a terpyridine-salicylaldehyde linked ligand (Figure 1b) and their metal complexes.

The ligand (tpyC5NHCOsalH) was prepared by condensation of 4-(2-(5-aminopentyloxy)phenyl)-terpyridine and 2-allyloxy-3-diethoxymethyl-5-methylbenzoic acid potassium salt (prepared by 6 steps and 4 steps from commercially avaiable material, respectively), followed by removing the allyl and diethyl acetal protecting groups (60% yield). The metal complexes (M^{2+} = Mn^{2+}, Fe^{2+}, Co^{2+}) were prepared by the reaction of the ligand with $[M(CH_3CN)_x](ClO_4)_2$ and 2,6-lutidine (1:1:2 in molar ratio) in CH_3CN. The ESI-MS spectra suggested 5-coordinate complexes, $[M(tpyC5NHCOsal)]^+$, were present in solutions.

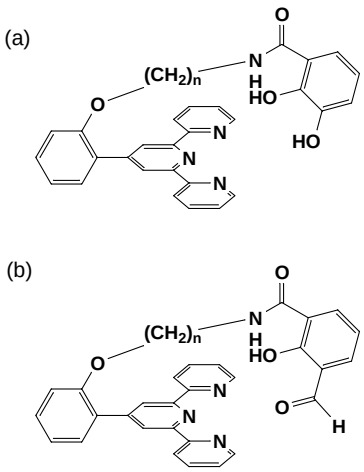

Figure 1. Terpyridine-based binary ligands.

VIII-H Development of Organic n-Type Semiconductors for Molecular Thin-Film Devices

Organic light-emitting diodes (OLEDs) and field-effect transistors (FETs) based on π-conjugated oligomers have been extensively studied as molecular thin-film devices. Organic n-type semiconductors (electron-transport materials) with low electron-injection barriers and high electron mobilities are required for highly efficient OLEDs and n-type FETs. Radical anions of an n-type semiconductor have to be generated easily at the interface with a metal electrode (electron injection), and electrons must move fast in the layer (electron mobility). Compared with organic p-type semiconductors (hole-transport materials), organic n-type semiconductors for practical use are few and rather difficult to develop. Recently, we found that perfluorinated phenylene dendrimers and oligomers are efficient electron-transport materials for OLEDs.

VIII-H-1 Synthesis, Characterization, and Electron-Transport Property of Perfluorinated Phenylene Dendrimers

SAKAMOTO, Youichi; SUZUKI, Toshiyasu; MIURA, Atsushi[1]; FUJIKAWA, Hisayoshi[1]; TOKITO, Shizuo[1]; TAGA, Yasunori[1]
([1]Toyota Central R&D Labs.)

[*J. Am. Chem. Soc.* **122**, 1832 (2000)]

Two perfluorinated phenylene dendrimers, $C_{60}F_{42}$ (MW = 1518) and $C_{132}F_{90}$ (MW = 3295), have been synthesized via a sequence of brominations and cross-couplings using organocopper chemistry. Two other $C_{60}F_{42}$ isomers containing *p*-terphenyl and *p*-quaterphenyl groups were also prepared to see structure-property relationships. Three $C_{60}F_{42}$s showed glass transitions at 125–135 °C. Dendrimer $C_{132}F_{90}$ melts at 426 °C and did not show a glass transition. Organic light-emitting diodes have been fabricated on indium-tin-oxide coated glass substrates by high-vacuum thermal evaporation of TPTE (a tetramer of triphenylamine) as the hole-transport layer, tris(8-quinolinolato)-aluminum as the emission layer, perfluorinated phenylenes as the electron-transport layer, LiF, and Aluminum. The maximum luminance of the device is 2860 cd/m^2 at 24.4 V. The electrochemical measurements indicated that the performance of the devices is improved with increasing electron affinities of the compounds. This is probably because the electron-injection barriers between the metal layers and the electron-transport layers are reduced by increased electron affinities.

VIII-H-2 Perfluorinated Oligo(*p*-Phenylene)s: Efficient n-Type Semiconductors for Organic Light-Emitting Diodes

HEIDENHAIN, Sophie; SAKAMOTO, Youichi; SUZUKI, Toshiyasu; MIURA, Atsushi[1]; FUJIKAWA, Hisayoshi[1]; MORI, Tomohiko[1]; TOKITO, Shizuo[1]; TAGA, Yasunori[1]
([1]Toyota Central R&D Labs.)

[*J. Am. Chem. Soc.* in press]

Perfluorinated oligo(*p*-phenylene)s including perfluoro-*p*-quinquephenyl to -octiphenyl (**PF–5P** to **–8P**) have been synthesized by the organocopper cross-coupling method. Two **PF–6P** derivatives containing trifluoromethyl and perfluoro-2-naphtyl groups were also prepared. All compounds are colorless solids and insoluble in common organic solvents. The differential scanning calorimetry measurements indicated that they are highly crystalline solids without glass transitions. Organic light-emitting diodes have been fabricated on indium-tin-oxide coated glass substrates by high-vacuum thermal evaporation of TPTE (a tetramer of triphenylamine) as the hole-transport layer, tris(8-quinolinolato)aluminum as the emission layer, a perfluorinated oligomer as the electron-transport layer, LiF, and aluminum. The electron-transport capabilities of perfluorinated oligo(*p*-phenylene)s are excellent compared with perfluorinated phenylene dendrimers. The maximum luminance of the naphtyl derivative is 19970 cd/m^2 at 10.0 V. The luminance-voltage and current-voltage characteristics of **PF–7P** and **–8P** are almost identical to those of **PF–6P**. We speculate that the electron mobility in the layer rather than the electron injection at the interface is responsible for determining the current density of **PF–6P** to **–8P**.

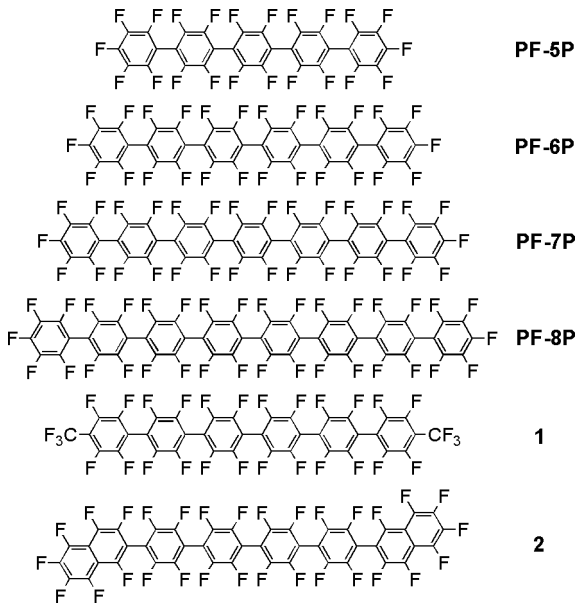

Figure 1. Perfluorinated phenylene oligomers.

VIII-I The Effects of the 2D Spin-Echo NMR Experiment on a Solid-State Homonuclear Sipn-1/2 Pair

The dipolar interaction for a solid-state homonuclear sipn-1/2 pair is averaged out by magic-angle sample spinning (MAS). The 2D spin-echo NMR experiment can reintroduce the influence of the homonuclear dipolar interaction into MAS powder signals.

VIII-I-1 Real Figure of Two-Dimensional Spin-Echo NMR Spectra for a Homonuclear Two-Spin System in Rotating Solids

KUWAHARA, Daisuke; NAKAI, Toshihito[1]; ASHIDA, Jun[2]; MIYAJIMA, Seiichi
([1]Tokyo Univ. Agric. Tech.; [2]Kyoto Univ.)

The 2D spin-echo NMR experiments were recently carried out on polycrystalline [2, 3-$^{13}C_2$] L-alanine under magic-angle sample spinning (MAS) conditions, so that two unusual resonance lines emerged along the F_1 axis (*Chem. Phys. Lett.* **305**, 35 (1999)). To examine a spectral structure observed in the F_1 direction more closely, we executed the 2D NMR experiment using a sufficiently small t_1 increment. As a result, we found many more resonance lines on a spectrum sliced off along the F_1 axis. The line distribution had a very unique and interesting structure. To elucidate the line positions theoretically, we calculated analytically the signals for the 2D spin-echo experiment performed with any t_1 increment on a homonuclear spin-1/2 pair undergoing MAS. We discovered that virtually six resonance lines (exactly twelve resonance lines) occurred on a spectrum sliced off along the F_1 axis. In addition, it was proved that the intensities of some resonance lines were largely dependent on the dipolar interaction.

VIII-J The Applications of Double-Rotation NMR Method

Double-Rotation NMR method (DOR) was applied to rare spins surrounded by abundant homonuclear spins. The application of the method to solid-state quadrupolar nuclei having $I = 1$ was investigated.

VIII-J-1 The Observation of REDOR Phenomenon for CH_x ($x \geq 2$) Spin Systems under DOR

KUWAHARA, Daisuke

Double-Rotation NMR method (DOR) was developed originally to remove second-order line broadenings for solid-state quadrupolar nuclei having half-integer spins. We applied the method to rare spins surrounded by abundant homonuclear spins (*i.e.* protons). DOR averaged out the homonuclear dipolar interactions, so that a CH_x system could be taken as an ensemble of independent CH systems. We could, therefore, detect heteronuclear dipolar interactions for CH_x ($x \geq 2$) spin systems without homonuclear decoupling techniques. In addition, we showed that DOR is also applicable to a solid-state ^{13}C-^{14}N spin pair in order to recover the heteronuclear dipolar interaction that was removed by sample spinning.